

Core Polarization and Quasiparticle Theories of Vibrational Nuclei with a Realistic Nucleon-Nucleon Force

M. GMITRO,* J. HENDEKOVIĆ,† AND J. SAWICKI

International Atomic Energy Agency, International Centre for Theoretical Physics, Trieste, Italy

(Received 5 December 1967)

Two- and four-quasiparticle Tamm-Dancoff theories are applied to study the even-parity states of the even tin isotopes. The residual nucleon-nucleon force is the realistic potential of Tabakin. We investigate the effects of the core neutrons and protons on our 0^+ , 2^+ , and 4^+ states by including the appropriate BCS and configuration-mixing contributions directly and by the "core polarization" renormalization of Bertsch, Kuo, and Brown. We find the core-polarization corrections most important and generally sufficient to explain the basic experimental data. The summation of the random-phase-approximation bubble and related exchange diagrams to all orders for the core nucleons gives almost the same results as those obtained with only second-order corrections. Such second-order corrections seem to be a sufficient approximation independently of the single-particle basis chosen.

1. INTRODUCTION

RECENTLY, Kuo and Brown¹ have proposed a method for deducing the effective interactions in finite nuclei from the so-called realistic potentials, i.e., those which reproduce the nucleon-nucleon scattering data. This method has then been applied to light nuclei in Ref. 1, by Kuo and Lynch² (O^{18} , F^{18} isotopes), and to studying the effective interactions in the nickel isotopes by Kuo.³ Another variant of the method has been studied by Bando.⁴

The method is based on treating excited configurations of the "inert" core nucleons through a renormalization of the matrix elements of the interaction between the "active" valence nucleons by second- and higher-order terms of the double and multiple scattering type. The method is in this sense related to multiple scattering terms in the Watson-Brueckner theory. However, the propagators are those of particle-hole pairs (3 particles and 1 hole intermediate states) since the essential process is that of a virtual excitation and a subsequent de-excitation of a core nucleon. This means calculating and summing mainly ring or "bubble" diagrams corresponding to an interaction of two valence nucleons through an intermediate third nucleon belonging to the core. A first calculation of this type has been published by Bertsch.⁵

In standard shell-model calculations with phenomenological nucleon-nucleon potentials or with adjustable reduced matrix elements to be determined from χ^2 fits to selected pieces of data, the effective forces already renormalized for the core-excitation effects are considered. This is by definition not the case with matrix

elements of a "bare" realistic nucleon-nucleon potential. Here at least an appropriate renormalization for a core "polarization" has to be sought if one is to justify a truncation of the single-particle spectrum allowing reasonable maximum dimensions of the Hilbert space for mixing all the important configurations of a given shell-model problem. In practice the shell-model single-particle space, i.e., the space of the valence ("active") subshells, is chosen to be that of all the subshells of the partly filled major shell immediately above a possibly doubly magic core which is the ensemble of all the completely filled (in the ground state) subshells.

In the following we concentrate on the spectroscopy of the even isotopes of tin of rather great interest both from the experimental and the theoretical point of view. In this case the active ("valence") subshells of neutrons only are commonly assumed to be $2d_{5/2}$, $1g_{7/2}$, $3s_{1/2}$, $2d_{3/2}$, and $1h_{11/2}$. We have chosen to investigate the effects of the underlying most important four subshells of the core $1g_{9/2}$, $2p_{1/2}$, $1f_{5/2}$, and $2p_{3/2}$, both of the neutrons and of the protons on the theoretical spectra determined in the Hilbert spaces based on the five valence subshells. Contributions of excitations to completely empty subshells above $1h_{11/2}$ (such as $1h_{9/2}$, etc.) can be shown to be much smaller. An analogous situation has been observed by Kuo³ in the nickel isotopes.

Completely prohibitive or even ridiculous dimensions of the exact shell-model Hilbert spaces in this case have forced us to choose the quasiparticle techniques which seem to be the only feasible ones in this region. The most important advantage of the method is that it accounts for the pairing correlations in a simple manner. The quasiparticle Tamm-Dancoff theories of the low-lying excited states of tin isotopes have proved very useful and apparently successful.⁶⁻⁸ While the simple

* On leave of absence from Nuclear Research Institute, Řež near Prague, Czechoslovakia.

† On leave of absence from Institute R. Bošković, Zagreb, Yugoslavia.

¹ T. T. S. Kuo and G. E. Brown, Nucl. Phys. **85**, 40 (1966); *ibid.* **A92**, 481 (1967).

² R. P. Lynch and T. T. S. Kuo, Nucl. Phys. **A95**, 561 (1967).

³ T. T. S. Kuo, Nucl. Phys. **A90**, 199 (1967).

⁴ H. Bando, report of work prior to publication; and International Conference on Nuclear Structure, Tokyo, 1967 (unpublished), contribution 4.30.

⁵ G. F. Bertsch, Nucl. Phys. **74**, 234 (1965).

⁶ R. Arvieu, Ann. Phys. (Paris) **8**, 407 (1963); R. Arvieu, E. Baranger, M. Vénéroni, M. Baranger, and V. Gillet, Phys. Letters **4**, 119 (1963).

⁷ P. L. Ottaviani, M. Savoia, J. Sawicki, and A. Tomasini, Phys. Rev. **153**, 1138 (1967); P. L. Ottaviani, M. Savoia, and J. Sawicki, Phys. Letters **24B**, 353 (1967); and (to be published).

⁸ T. T. S. Kuo, E. Baranger, and M. Baranger, Nucl. Phys. **79**, 513 (1966).

two-quasiparticle Tamm-Dancoff (QTD) theory proves to be a reasonable approximation, at least for the first excited 2_1^+ and 4_1^+ states of the even tin isotopes, one should include four-quasiparticle admixtures of a quasiparticle second Tamm-Dancoff (QSTD) approximation in order to account for the lowest-lying 0^+ states of the same nuclei.⁷

We have chosen three parallel lines of calculation to compare their respective results in connection with the case described above.

In the first series of calculations we apply just the "bare," unrenormalized elements of our realistic nucleon-nucleon potential to QTD (and QSTD for the 0_n^+ states) calculations of the even parity states of the even tin isotopes including the five valence subshells of the neutrons only, i.e., excluding the core.

In the second series we perform QTD calculations only (unfortunately the QSTD dimensions become prohibitive, in this case, even for the 0_n^+ states) again with the same "bare" matrix elements, but in a space of single-particle levels including the four core subshells both for the neutrons and for the protons. In this case we have, altogether, nine neutron and nine proton single-particle levels explicitly involved in the configuration mixing.

Finally, in our third series, we redo our QTD (and QSTD for the 0_n^+) calculations with only the five valence neutron subshells but with the matrix elements of the same realistic force renormalized for including the core polarization corresponding to virtual particle-hole pairs of the neutrons and protons which belong to the four core subshells indicated above. The said core polarization is treated by (a) the formulas given by Kuo and Brown¹ and by Kuo³ and (b) including the sums of all the usual random-phase-approximation (RPA) particle-hole ring ("bubble") diagrams of the core nucleons. A treatment similar to (b) has already been proposed by Bando.⁴ In addition, we mention some other possible variants of the above theoretical models.

Our realistic nucleon-nucleon interaction potential is that of Tabakin.⁹ It is a superposition of nonlocal separable components for the partial waves S , P , and D which reproduces the experimental nucleon-nucleon scattering data up to 320 MeV. Recently, this potential has been applied to nuclear-structure calculations and proved quite successful in most respects. Kerman *et al.*¹⁰⁻¹² have performed extensive and successful Hartree-Fock calculations on several nuclei with this potential. They find rather important second-order corrections¹² and this is generally consistent with our findings.

⁹ F. Tabakin, *Ann. Phys. (N. Y.)* **30**, 51 (1964).

¹⁰ A. K. Kerman, J. P. Svenne, and F. M. H. Villars, *Phys. Rev.* **147**, 710 (1966).

¹¹ W. H. Bassichis, A. K. Kerman, and J. P. Svenne, *Phys. Rev.* **160**, 746 (1967).

¹² A. K. Kerman and M. K. Pal, *Phys. Rev.* **162**, 970 (1967).

Kuo *et al.*¹³ have obtained, with the use of the potentials of Tabakin, a satisfactory agreement with the experimental odd-even mass difference and with the low-energy spectra of the odd tin isotopes and with the corresponding changes in separation energies. Barrett¹⁴ has applied Tabakin potentials to spectroscopic calculations for the α particle and for the O^{16} nucleus.¹⁵ Hodgson¹⁶ applies the same potentials to study the spectra of O^{18} and F^{18} , and Gambhir and Ram Raj¹⁷ apply it to their exact shell-model calculations in Ni^{58} and Ni^{60} . The agreement with the data in the latter case is not very good just because the calculation of Ref. 16 employs only the "bare" elements of Tabakin's potential in a very restricted subspace of only three valence subshells.

Elliott *et al.*¹⁸ derive reduced shell-model matrix elements of the two-body nuclear force directly from the experimental phase shifts and find that they are close to the corresponding elements of the Tabakin potential.

In Sec. 2 we present in detail the various different variants of the theory of the core polarization effects together with their discussion.

In Sec. 3 we review very briefly the essentials of our treatment of the pairing interaction and of the quasiparticle Tamm-Dancoff approximations and give our numerical results for our three parallel theoretical models as described above.

Section 4 contains a final discussion of our results and conclusions.

2. THEORY OF CORE POLARIZATION CORRECTIONS

The quasiparticle Tamm-Dancoff theories employ in mixing configurations both the particle-hole and the particle-particle type coupled reduced matrix elements. This formal complication arises from the Bogolyubov-Valatin canonical transformation.

Such elements have been defined, e.g., by Baranger¹⁹; in the following we use most of his notations. Greek letters are reserved for all quantum numbers, including the magnetic number of the single-particle state, while the corresponding latin letters denote the same with the exclusion of the magnetic number. The symbol U stands for the antisymmetrized two-body potential operator $U=V(1,2)(1-P_{12})$ where P_{12} exchanges 1 and 2.

¹³ T. T. S. Kuo, E. Baranger, and M. Baranger, *Nucl. Phys.* **81**, 241 (1966).

¹⁴ B. R. Barrett, *Phys. Rev.* **154**, 955 (1967).

¹⁵ B. R. Barrett, *Phys. Rev.* **159**, 816 (1967).

¹⁶ R. J. W. Hodgson, *Phys. Rev.* **156**, 1173 (1967).

¹⁷ Y. K. Gambhir and Ram Raj, *Phys. Rev.* **161**, 1125 (1967).

¹⁸ J. P. Elliott, H. A. Mavromatis, and E. A. Sanderson, *Phys. Letters* **24B**, 358 (1967). An even better agreement with their matrix elements is obtained when one includes the second-order polarization corrections to the Tabakin potential—E. Baranger (private communication via D. M. Brink).

¹⁹ M. Baranger, *Phys. Rev.* **120**, 957 (1960).

Introducing the isotopic spin, we can write

$$\begin{aligned} & \langle \alpha\beta | U | \gamma\delta \rangle \\ &= -2 \sum_{J'M'T'M_T'} G(abcdJ'T') (j_a j_b m_\alpha m_\beta | J'M') \\ & \quad \times (j_c j_d m_\gamma m_\delta | J'M') \left(\frac{1}{2} \frac{1}{2} t_a t_b | T'M_T'\right) \\ & \quad \times \left(\frac{1}{2} \frac{1}{2} t_c t_d | T'M_T'\right), \quad (1) \end{aligned}$$

$$\begin{aligned} & \langle \alpha\beta | U | \gamma\delta \rangle \\ &= -2 \sum_{J''M''T''M_T''} F(acdbJ''T'') \\ & \quad \times s_\beta s_\gamma (j_a j_c m_\alpha - m_\gamma | J''M'') \\ & \quad \times (j_d j_b m_\delta - m_\beta | J''M'') (-)^{l-b-t_c} \\ & \quad \times \left(\frac{1}{2} \frac{1}{2} t_a - t_c | T''M_T''\right) \left(\frac{1}{2} \frac{1}{2} t_d - t_b | T''M_T''\right), \quad (2) \end{aligned}$$

where $s_\pi \equiv (-)^{j_\pi - m_\pi}$. The symbols $G(abcdJ'T')$ and $F(acdbJ''T'')$ are just the particle-particle and particle-hole type reduced matrix elements in the notation analogous to that of Baranger.¹⁹ The G , $F(abcdJT)$ satisfy several simple and obvious symmetry relations.

Kuo and Brown¹ and Kuo³ have given explicit formulas for the second-order core polarization corrections for elements with the particle-particle type vector couplings:

$$\langle abJT | K(q/e)K | cdJT \rangle = N_{cd}{}^{ab} \Delta^{(2)} G(abcdJT). \quad (3)$$

Here $N_{cd}{}^{ab} \equiv -2(1 + \delta_{ad})^{-1/2}(1 + \delta_{cb})^{-1/2}$ is a normalization constant, and $\Delta^{(2)} G(abcdJT)$ is the core polarization correction to the corresponding $G(abcdJT)$ computed with the antisymmetrized K operator. Here the K operator is the Brueckner reaction matrix; it corresponds to our U defined above: One must work with such reaction matrix operators in the case of singular (hard-core type) realistic nucleon-nucleon potentials. In the case of nonlocal potential of the Tabakin type one can utilize the U approximation: In fact, it has been shown by Hodgson¹⁶ that spectroscopic predictions obtained with the K matrix of the Tabakin potential are almost the same as those obtained with the corresponding "bare" U elements.

The second-order corrections of Refs. 1 and 3 include all the antisymmetrized (both direct and all exchange) diagrams involving three-particle and one-hole lines in the intermediate states, and not only the simplest RPA bubble diagrams, but they exclude the obvious self-energy type second-order bubble corrections which should be included already in the zero-order Hartree-Fock shell-model energies. Their propagator q/e , where q projects out the particle-hole pairs and e is the energy denominator, is slightly simplified by approximating e by only the particle-hole excitation energy, $e = E_p^0 - E_h^0$, in our notations.

The formula for the correction $\Delta^{(2)} F(acdbJT)$ to the first-order $F(acdbJT)$ coming from the very same second-order diagrams of the core polarization is much

simpler because of more natural vector couplings in line with the particle-hole projector in this case.

The transformation from G to F is readily defined as

$$\begin{aligned} F(acdbJT) &= - \sum_{J'T'} \hat{J}^2 \hat{T}^2 W(j_a j_b j_c j_d; J'J) \\ & \quad \times W\left(\frac{1}{2} \frac{1}{2} \frac{1}{2} \frac{1}{2}; T'T\right) G(bacdJ'T'), \quad (4) \end{aligned}$$

where $\hat{J} = (2J+1)^{1/2}$.

Utilizing Eq. (1) of Kuo,³ performing the transformation of Eq. (4), and avoiding the above-mentioned simplification of the denominators e , we easily arrive at the following formula for the second-order core polarization correction to $F(acdbJT)$

$$\begin{aligned} \Delta^{(2)} F(acdbJT) &= I(acdbJT) \\ & + (-)^{J+T} \sum_{J'T'} \hat{J}^2 \hat{T}^2 \left\{ \begin{matrix} j_a & j_c & J \\ j_b & j_d & J' \end{matrix} \right\} \left\{ \begin{matrix} \frac{1}{2} & \frac{1}{2} & T \\ \frac{1}{2} & \frac{1}{2} & T' \end{matrix} \right\} (-)^{J'+T'} \\ & \times [(-)^{j_c+j_d} I(adcbJ'T') + (-)^{j_a+j_b} I(bcdaJ'T')] \\ & + (-)^{j_a+j_b+j_c+j_d} I(bdcaJT), \quad (5) \end{aligned}$$

where

$$\begin{aligned} I(abcdJT) &= \frac{1}{2} \sum_{ph} N_{bp}{}^{ah} N_{dp}{}^{ch} F(abphJT) (q/e) F(phcdJT). \end{aligned}$$

In the above expression the propagator q/e to the left of an element $F(phss'JT)$ contains $e \equiv [(E_p^0 - E_h^0) - (E_s^0 - E_{s'}^0)]$, where h stands for the hole state, p for the particle state of the third (core) nucleon involved, and s, s' belong to the valence shells; E_k^0 denotes the single-particle shell-model (Hartree-Fock) energy.

The four terms of Eq. (5) represent four different basic second-order processes with all the exchanges between the pairs involved. These pairs are the nucleons "1 and 3" and "2 and 3," respectively, and the corresponding F elements are antisymmetrized just in these respective pairs. The terms second and third represent the exchange $c \leftrightarrow d$ and $a \leftrightarrow b$ terms relative to the first and the last terms; this means actually antisymmetrization in the nucleons "1 and 2" of the basic terms: first and fourth. To understand the physical meaning of these two fundamental terms, let us examine their respective direct parts [in (1,3) and (2,3), respectively]. The corresponding two Feynman diagrams are given in Fig. 1. We see that the diagram (2) is the RPA

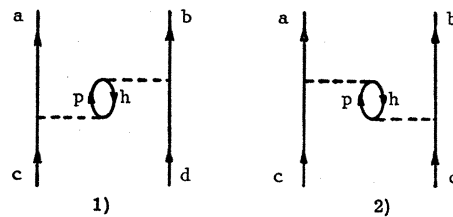


FIG. 1. Second-order bubble diagrams of core polarization corresponding to the terms 4th and 1st of the right-hand side of Eq. (5).

“backward-going” (or de-excitation) graph relative to the first one. Analogous diagrams are much less important in problems involving only pure particle-hole interactions of an RPA treatment of a nonsuperconducting (normal state) nucleus. In our case the propagator associated with the first diagram could be written as

$$q \cdot [(E_p^0 - E_h^0) - (E_c^0 - E_a^0)]^{-1},$$

while that of the diagram (2) of Fig. 1 is

$$q \cdot [(E_p^0 - E_h^0) - (E_d^0 - E_b^0)]^{-1}.$$

In a typical RPA calculation for a light nucleus, one of the two $d \leftrightarrow b$ and $c \leftrightarrow a$ lines is a hole line and the other a particle line. In such a situation $E_c^0 - E_a^0$ would be negative if, e.g., $E_d^0 - E_b^0$ were positive. Consequently the diagram (2) of Fig. 1 would be more important (smaller energy denominator) than the diagram (1). This is generally not the case in our problem of a, b, c, d belonging to the five valence subshells of the tin isotopes (h refers to the four underlying core subshells). Actually Refs. 1 and 3 even suppress the excitations $E_d^0 - E_b^0$ and $E_c^0 - E_a^0$ as numerically small relative to $E_p^0 - E_h^0$ (in their cases $E_p^0 - E_h^0$ is of the order of $2\hbar\omega_0$ of the harmonic oscillator).

It seems important to investigate the effect of all the higher-order RPA bubble diagrams. This is particularly interesting as one wonders about the convergence of such series of core polarization corrections in cases where those of the second order are already quite large. Also, the Tabakin potentials are known to have large second-order matrix elements.

The summation of the all the RPA-type bubble diagrams with all the exchanges can be performed by solving by iteration the integral equation

$$\mathfrak{F}(acdbJT) = F(acdbJT) + \Delta F(acdbJT)[\mathfrak{F}], \quad (6)$$

where $\Delta F(acdbJT)[\mathfrak{F}]$ differs from $\Delta^{(2)}F(acdbJT)$ of Eq. (5) by the replacement of the $F(phcdJT)$ standing to the right in the definition of $I(abcdJT)$ with the corresponding \mathfrak{F} element. This procedure we have applied, and we compare all our corresponding quasi-particle Tamm-Dancoff results for the Sn isotopes with the simpler case where only the second-order polarization corrections are included, i.e., where the $G, F(acdbJT)$ elements are replaced by

$$G + \Delta^{(2)}G, F + \Delta^{(2)}F(acdbJT).$$

In this connection we may mention the calculations by Bando,⁴ in which he solves the integral equation

$$\mathfrak{F}(acdbJ) = F(acdbJ) + 2 \sum_{xx'=(ph \text{ or } hp)} F(acxx'J)(\tilde{q}/e)\mathfrak{F}(xx'dbJ). \quad (7)$$

Bando works with neutron pairs only, and he does not couple to states of a definite isotopic spin T . His antisymmetrized pair states are not normalized as those in Refs. 1-3 and in the present paper (the corresponding

terms differ whenever we encounter an F element corresponding to a pair $|aaJ\rangle$ from the same subshell). Further, Bando's second term on the right-hand side of Eq. (7) corresponds approximately to only the first and fourth term on the right-hand side of Eq. (5) or the corresponding terms in Eq. (6). Thus Bando's iteration includes fewer classes of diagrams than that of our Eq. (6).

As for the propagators \tilde{q}/e , Bando chooses an average occupation of $\frac{1}{2}$ in the valence (open) subshells, i.e., he has $\tilde{q} = \frac{1}{2}$ when $(xx') = (ph)$ and $\tilde{q} = -\frac{1}{2}$ when $(xx') = (hp)$. This *Ansatz* is not unreasonable in cases such as that of Sn where an average occupation of the five valence neutron subshells is $(N-50)/32$, i.e. $= \frac{1}{2}$ for the 116 isotope with the neutron number $N=66$.

In our calculations, the results of which we present below, we have considered several assumptions for the propagators q/e . First we consider several different possible choices of the shell-model (Hartree-Fock) single-particle energies $\{E_s^0\}$ for our (complete) energy denominator e .

As for the q projector, we consider two cases: (1) $q = +1$ for all the ph cases where h belongs to the four core subshells and p to any one of the valence subshells for the protons and the neutron p can be only the (highest) $1h_{11/2}$ subshell; this is not unreasonable in cases such as Sn¹²⁰ where, in the absence of any pairing effect, the $1h_{11/2}$ level would be quite free and all the lower ones quite occupied in the ideal simplest shell model; finally, (2), $q = \tilde{q}$ of Bando⁴ for the neutron (ph) pairs (i.e., $= \frac{1}{2}$) and q is the same as case (1) for the protons.

We compare and discuss below consequences of these different *Ansätze*.

A simpler variant of this theory (and an approximately reasonable one, it seems) would arise if we include in $\Delta F(acdbJT)[\mathfrak{F}]$ of Eq. (6) only what corresponds to iterating the first and the last of the four terms of Eq. (5). This would mean not antisymmetrizing explicitly in the particles 1 and 2 the second- and higher-order polarization corrections.

As for the isotopic spin (T) coupling, we may mention the following general relations which enable re-writing our Eqs. (5)-(6) in the language of pairs with definite nucleonic charges $\nu \equiv$ neutron, $\pi \equiv$ proton:

$$G(a_\nu b_\nu c_\nu d_\nu J) = G(abcdJ \ T=1), \quad (8)$$

$$G(a_\pi b_\nu c_\pi d_\nu J) = \frac{1}{2}[G(abcdJ \ T=0) + G(abcdJ \ T=1)], \quad (9)$$

$$F(a_\nu c_\nu d_\nu b_\nu J) = \frac{1}{2}[F(acdbJ \ T=0) + F(acdbJ \ T=1)], \quad (10)$$

$$F(a_\pi c_\pi d_\nu b_\nu J) = \frac{1}{2}[F(acdbJ \ T=0) - F(acdbJ \ T=1)], \quad (11)$$

and the same with π interchanged with ν . Equations (8)-(11) are useful for cases where the respective neutron and proton particle-hole spaces are different.

TABLE I. Single-particle energies $\{E_s^0\}$ (in MeV) of Sn^{116} : (1) The sets labeled Bando 1 and 2 are based on Ref. 4, (2) the sets labeled BEL 1 and 2 are based on Ref. 20, and (3) the set labeled KBB is the set "Tab. 1" of Table 7 of Ref. 13.

$\{E_s^0\} \backslash nj$	$2d_{5/2}$	$1g_{7/2}$	$3s_{1/2}$	$2d_{3/2}$	$1h_{11/2}$	$1g_{9/2}$	$2p_{1/2}$	$1f_{5/2}$	$2p_{3/2}$
Bando 1	0.0	0.40	1.90	2.20	2.40	-4.0	-12.0	-12.0	-12.0
Bando 2	0.0	0.40	1.90	2.20	2.40	-4.0	-9.0	-9.0	-9.0
BEL 1	0.0	0.305	2.048	2.179	2.702	-4.0	-12.0	-12.0	-12.0
BEL 2	0.0	0.305	2.048	2.179	2.702	-4.0	-9.0	-9.0	-9.0
KBB	0.0	0.3	1.5	2.15	3.45	-2.5	-4.0	-5.0	-5.5

3. QUASIPARTICLE TAMM-DANCOFF CALCULATIONS OF THE EVEN PARITY STATES OF EVEN TIN ISOTOPES AND THE EXCITATIONS OF THE CORE NUCLEONS

Our single-particle basis should be ideally constructed from a self-consistent Hartree-Fock-Bogolyubov procedure with our Tabakin potentials. This has not been achieved and it is a formidable task in itself and essentially outside the scope of the present paper. Such effort would be necessary if a serious attempt to obtain a quantitative fit to the existing experimental data were to be made.

A treatment of the "superconductive" effects of the BCS pairing interactions already in the construction of our basis is well known to be necessary in the case of tin isotopes.

We obtain our BCS solutions for the neutron and proton subshells from several sets of phenomenological "unperturbed" (zero-order) shell-model single-particle energies $\{E_s^0\}$ which are taken from the literature. Except when specified, we include in all the cases the Hartree-Bogolyubov self-energy corrections μ_s of the residual interaction potential.

In the following we present and compare our results for several examples of sets of $\{E_s^0\}$ given in Table I. The motivation for our choice was a relatively wide variation of the single core nucleon energies between these sets and reasonable level sequences and densities. Our harmonic-oscillator radial wave functions correspond to the value $\hbar\omega_0 = 41A^{-1/3}$ MeV with $A = 116$.

With the sets $\{E_s^0\}$ of Table I we solve the BCS equations finding the single qp energies

$$E_s = [(E_s^0 + \mu_s - \lambda)^2 + \Delta_s^2]^{1/2}.$$

In the case of protons they practically (in some cases exactly) reduce the normal-state solutions (zero gaps). In the following we also consider the case where we assume zero energy gaps for the four core neutron levels, i.e., where the corresponding "hole"-qp energies reduce to appropriate $|E_s^0 + \mu_s - \lambda|$.

We apply the QTD and QSTD approximations of Refs. 6-7 to calculate the lowest few excited states 2^+ , 4^+ , and 0^+ of the "typical" two isotopes of tin with $A = 116$ and 120. The same Tabakin potentials which are used to determine our BCS single-qp solutions are now used to mix our excited two-qp (or zero-, two-, and

four-qp) configurations. Our explicit formulas for the reduced G - and F -matrix elements for Tabakin's potentials are the same or equivalent to those given in Refs. 13-17. We have utilized the computer FORTRAN codes of Ref. 7 for QSTD and slightly modified programs for our QTD problems. The 0^+ states are obtained from diagonalizations of secular matrices after the elimination of the spurious ket $\mathcal{H}_n(\tilde{N}_n - N_{0n})|0\rangle$ (and of $\mathcal{H}_p(\tilde{N}_p - N_{0p})|0\rangle$ if necessary) in the QTD case, of the same neutron ket and of six higher-order spurions described in Ref. 7 in the QSTD case (seven 0^+ spurions). Here $|0\rangle$ stands for the qp vacuum; $\tilde{N}_{n(p)}$ is the neutron (proton) number operator, and $N_{0n(p)}$ is the actual number of interacting neutrons (protons). The spurions are projected out of our secular matrices by a Schmidt procedure. There are no similar spurions to be projected out for $J^\pi = 2^+, 4^+$ in the QTD approximation.

Our 0^+ , 2^+ , and 4^+ lowest eigenvalues for $A = 116$ calculated with "bare" matrix elements of the Tabakin potential and mixing only the configurations belonging to the five neutron valence subshells are presented in Table II. The ground state (0_1^+) has, by definition, energy zero in the QTD approximation ($|0\rangle$). In the QSTD problem it has four-qp correlations, and is lowered in energy relative to $|0\rangle$ (a negative energy shift). The percentages of the four-qp components (% 4-qp) are indicated in parenthesis for each QSTD 0^+ state. The 4-qp weights of the states $0_{2,3}^+$ are surprisingly small here. The 0^+ QSTD secular matrices have the dimensions 56×56 .

TABLE II. QTD and QSTD energy eigenvalues (in MeV) of the 0^+ , 2^+ , and 4^+ states of Sn^{116} calculated with the bare matrix elements of the Tabakin potential and with the five neutron valence subshells only; the sets $\{E_s^0\}$ are those of Table I (no distinction is needed here between the subsets 1 and 2 of Table I). The four-qp percentages of the QSTD eigenvectors $|0_n^+\rangle$ are indicated in parentheses.

$\{E_s^0\} \backslash J^\pi$	0^+	2^+	4^+
	QTD	QSTD (% 4qp)	QTD
Bando	0.0	-0.02(35.9)	1.27
	1.54	1.43(4.6)	2.00
	2.22	2.10(6.4)	2.20
BEL	0.0	-0.04(36.0)	1.28
	1.52	1.40(5.2)	1.94
	2.09	1.88(13.1)	2.17
KBB	0.0	-0.07(36.9)	1.18
	1.46	1.43(3.9)	1.60
	1.74	1.85(15.3)	1.83

The observed level energies (in MeV) of Sn^{116} are as follows: 0_2^+ , 1.762; $2_{1,2}^+$, 1.291 and 2.108; $4_{1,2}^+$, 2.391 and 2.531. While it is not our aim to fit the experimental data in the present calculations, we may make several general remarks concerning this point and Table II. Agreement with the observed energies is, on the average, rather poor for all the sets of $\{E_s^0\}$ considered. In particular, the 4^+ levels come down much too low and this resembles the difficulty encountered in exact shell-model calculations in the even Ni isotopes.²⁰ Our set BEL is the best in Table II.

The negative of the QSTD ground-state energy shift could be added to the excitation energies [e.g., $E(0_2^+) = 1.40 + 0.04 = 1.44$ MeV, etc.]. This, however, is quantitatively unreliable for the reasons discussed in Ref. 7, in particular, because of the lack of a Hartree-Fock-Bogolyubov self-consistency in our calculations.

The same trends are found in the isotopes 120 and 124. Generally, for higher A , the level 0_2^+ rises and the levels 2_1^+ and 4_1^+ become lower. For example, for $A = 120$ we find in QTD: (a) for the $\{E_s^0\}$ due to KBB⁸ (0_2^+ , 1.71; 2_1^+ , 1.12; and 4_1^+ , 1.50 MeV); (b) for the set due to BEL²¹ (0_2^+ , 1.46; 2_1^+ , 1.02; and 4_1^+ , 1.45 MeV), as compared with the experimental energies: 0_2^+ , 1.872; 2_1^+ , 1.166; and 4_1^+ , 2.183 MeV. The general trend of the variation with A is then qualitatively reproduced but the calculated 4_1^+ are much too low. This was not the case with the results of Ref. 7 obtained with unrealistic two-body forces. On the other hand, we cannot hope for a reliable quantitative fit with the present approximations. Also, our aim is to study the effect of core excitation with a realistic potential rather than just to try to explain existing data.

In our second series we perform slightly modified QTD calculations now in Hilbert spaces, corresponding to all the nine single-particle levels of Table I for both the neutrons and the protons. Again only 0^+ , 2^+ , and 4^+ states are calculated for $A = 116$ and 120 and the matrix elements of the Tabakin potential are "bare."

Here we consider two cases. In the first one only the five valence neutron subshells are "superconducting," all the others are of normal state, i.e., without the energy gaps; similarly we keep in the configuration mixing in this case only pure particle-hole proton pairs. With our particular nine subshells the new excited configurations contribute nothing to the 0^+ levels (are decoupled from the basic configurations) so that the QTD results for 0^+ here are the same as those of Table II. In the second case the BCS pairing effect is extended to include the four core neutron subshells (and to all the proton subshells). This changes the single-qp energies in a very important way and therefore also the QTD 0^+ eigenvalues, although here again the extra configuration mixing effect is negligible. Obviously,

spurious components corresponding to Cooper pairs in the limit of normal state are practically uncoupled from the other components in the physically meaningful eigenvectors.

Our QTD 0^+ , 2^+ , and 4^+ levels for both these cases are given for $A = 116$ in Table III.

The 2^+ and 4^+ QTD levels are slightly lowered in our first case in relation to those of Table II because of the extra configuration mixing.

In the second case, the strength of the BCS pairing effect is typically rather exaggerated, which also results in typically too high 0^+ excited states (BEL 1, Bando 1). The 2_1^+ level also lies too high. Our 4_1^+ level is the best for the KBB case in this variant of our QTD model.

In order to examine properly all the important effects of the extra configurations arising from the inclusion of the extra four neutron- and the nine proton subshells one would have to solve at least the corresponding full QSTD secular problems. Unfortunately, the enormous dimensions of such secular matrices are quite prohibitive and far beyond the capacities of the present-day computers. It is for this reason that, unfortunately, we cannot consider the results of Table III as representative of all the most important effects of the extra configuration mixing which should be reproduced in the core polarization calculations reported below.

In our third series we present a number of results on the 0^+ , 2^+ , and 4^+ levels as calculated with the core polarization corrections included and the excited configurations appropriate to the five neutron subshells only.

In order to study the most delicate question of the effects of the details of the energy denominators of our propagators q/e in Eqs. (5)–(6), we have considered four cases in detail: the case labeled S1 means a simplification in which only the p - h excitation energy $E_p^0 - E_h^0$ is retained in e , while q admits neutron particles (p) only in the $1h_{11/2}$ subshell; the case labeled S2 differs from the previous one only by using the Bando ($q = +\frac{1}{2}$ for ph) assumption; in the cases labeled

TABLE III. QTD energies (in MeV) of the 0^+ , 2^+ , and 4^+ states of Sn^{116} calculated with the bare matrix elements of the Tabakin potential and with the nine neutron and proton subshells of Table I ($\{E_s^0\}$) of Bando 1, BEL 1, and KBB; a distinction is made between the 2^+ and 4^+ results obtained with and without the BCS pairing effect for the four neutron core subshells.

$\{E_s^0\} \backslash J^\pi$	BCS for valence neutrons only		BCS for 9+9 levels		
	2^+	4^+	0^+	2^+	4^+
Bando 1	1.22	1.83	0.0	1.37	1.86
			2.09		
BEL 1	1.96	2.17	2.94	2.50	2.92
	1.20	1.83	0.0	1.33	1.64
			2.00		
KBB	1.87	2.13	2.80	2.35	2.91
	1.10	1.55	0.0	1.57	2.18
			1.44		
	1.58	1.79	2.58	2.03	2.55

²⁰ S. Cohen, R. D. Lawson, M. H. MacFarlane, S. P. Pandya, and M. Soga, Phys. Rev. **160**, 903 (1967).

²¹ B. L. Birbrair, K. I. Erokhina, and I. Kh. Lemberg, Izv. Akad. Nauk SSSR Ser. Fiz. **27**, 150 (1963).

C1 and C2 the full denominator e is retained and q is that of the cases S1 and S2, respectively.

The effects of the corrections in question are twofold in the case of superconductive nuclei in contrast to those in the normal state. In fact, the changes in the effective pairing force, i.e., in the calculated energy gaps and the chemical potentials, are even more important than the changes in the effective residual interaction responsible for the configuration mixing.

In Table IV we give an example of this effect on the five neutron single-qp energies: the isotope is $A=116$, and the set $\{E_s^0\}$ is that of Bando 1 giving in our S2 treatment of the second-order core polarization the spectrum of 0^+ , 2^+ , and 4^+ closest to the observed levels. We compare our $\{E_s\}$ of the BCS solution with the "bare" pairing Hamiltonian of the Tabakin potential with those where the second-order core polarization is also included.

We see that indeed the enhancement of our E_s due to the core polarization is quite impressive.

In Tables V and VI we compare with each other all the mentioned cases for $A=116$ on the QTD (and

TABLE IV. Single quasiparticle energies E_s (in MeV) calculated for the five neutron valence subshells with the bare and with the renormalized matrix elements of the BCS pairing force of the Tabakin potential; the unperturbed energies E_s^0 are those of Bando 1 of Table I.

pairing force \ nlj	$2d_{5/2}$	$1g_{7/2}$	$3s_{1/2}$	$2d_{3/2}$	$1h_{11/2}$
bare	1.91	1.21	1.10	1.08	1.04
core pol. incl.	2.03	1.68	1.32	1.48	1.28

QSTD) 0^+ , 2^+ , and 4^+ levels. In the 0^+ QSTD cases we give (in parentheses) the 4-qp percentages of the corresponding eigenvectors.

The case labeled IS2 means "iterated" S2, i.e., where the core polarization corrections are taken to all orders by solving the integral Eq. (6) by iterations [the corresponding values of $G+\Delta G$ are obtained from Eq. (4)]. This is done only in the S2 case. We see (cf. also Fig. 2) that the case IS2 where all the RPA bubble diagrams (cf. Fig. 3), both for the core neutrons and protons and all the related exchange diagrams, are included differs only by negligible shifts from the corresponding cases S2 where only the second-order bubble and related diagrams are retained. It is for this reason that we have limited ourselves for IS2 to two cases of $\{E_s^0\}$ only Bando 1 and KBB in our QTD calculations, and we have left out the IS2 variant from our QSTD part altogether.

We stress the importance of the result that the second-order core polarization corrections are actually a sufficient approximation. In particular, we remark that this feature remains valid also in the cases where the average energy separation of the core subshells from the valence subshells is small (KBB), i.e., seems not to depend on the choice of $\{E_s^0\}$.

TABLE V. QTD and QSTD energy eigenvalues (in MeV) of the $0_{1,2,3}^+$ states of Sn^{116} calculated with the Tabakin potential with the core polarization included for the five sets of E_s^0 of Table I; the labels C and S refer to the "complete" [$e=(E_p^0-E_h^0)-(E_s^0-E_s^0)$] and to the "simplified" ($e=E_p^0-E_h^0$) energy denominators in the core polarization corrections, respectively; the labels 1 and 2 refer to the two different choices of the p - h projector q for the neutron p - h pairs as described in the text; the case IS2 includes the core polarization diagram of the type S2 to all orders. The four-qp percentages of the QSTD eigenvectors $|0_n^+\rangle$ are indicated in parentheses.

$\{E_s^0\}$			QTD			QSTD
	C1	C2	S1	S2	IS2	S2
Bando 1	0.0	0.0	0.0	0.0	0.0	-0.07(36.0)
	2.28	2.19	2.10	2.05	2.09	1.94(4.2)
	3.28	3.27	2.91	2.90	2.92	2.76(5.4)
Bando 2	0.0	0.0	0.0	0.0		-0.05(36.0)
	2.33	2.24	2.14	2.10		1.98(4.6)
	3.32	3.31	2.93	2.92		2.73(9.8)
BEL 1	0.0	0.0	0.0	0.0		-0.07(35.9)
	2.29	2.19	2.07	2.03		1.90(5.0)
	3.24	3.23	2.82	2.80		2.58(11.8)
BEL 2	0.0	0.0	0.0	0.0		-0.08(36.0)
	2.34	2.24	2.11	2.07		1.94(4.8)
	3.28	3.25	2.84	2.82		2.60(11.3)
KBB	0.0	0.0	0.0	0.0	0.0	-0.28(37.6)
	3.38	3.15	2.61	2.54	2.65	2.68(19.1)
	5.29	5.18	3.00	2.89	2.97	2.84(6.4)

In Fig. 4 we give a comparison of our results of Tables V and VI for the set BEL 1 with our corresponding previous results of Tables II and III and with experiment all for the Sn^{116} nucleus. The QSTD levels $0_{1,2}^+$ are indicated by dashed lines.

A similar comparison is given in Fig. 5 for the 120 isotope.

Important tests of semiquantitative validity of microscopic models such as our present ones are the predicted electromagnetic transition probabilities and static moments. For the even tin isotopes there exist already quite a few pieces of data on the $B(E2, I_i \rightarrow I_f)$

TABLE VI. QTD energies (in MeV) of the $2_{1,2}^+$ and $4_{1,2}^+$ states calculated with the Tabakin potential with the core polarization included for all the cases explained in Table V.

$\{E_s^0\}$	J_n^τ	C1	C2	S1	S2	IS2
Bando 1	2_1^+	1.52	1.44	1.48	1.44	1.46
	2_2^+	2.85	2.82	2.64	2.62	2.65
	4_1^+	2.40	2.32	2.33	2.27	2.29
	4_2^+	3.04	2.97	2.86	2.81	2.85
Bando 2	2_1^+	1.57	1.50	1.52	1.48	
	2_2^+	2.90	2.87	2.68	2.66	
	4_1^+	2.46	2.38	2.36	2.31	
	4_2^+	3.09	3.02	2.90	2.85	
BEL 1	2_1^+	1.53	1.45	1.48	1.44	
	2_2^+	2.84	2.80	2.61	2.57	
	4_1^+	2.45	2.35	2.26	2.29	
	4_2^+	3.04	2.97	2.84	2.79	
BEL 2	2_1^+	1.59	1.51	1.52	1.48	
	2_2^+	2.90	2.85	2.64	2.61	
	4_1^+	2.51	2.41	2.39	2.33	
	4_2^+	3.10	3.01	2.88	2.82	
KBB	2_1^+	1.96	1.65	1.63	1.54	1.57
	2_2^+	4.28	3.92	2.96	2.83	2.91
	4_1^+	3.64	3.31	2.70	2.61	2.69
	4_2^+	4.35	3.96	3.33	3.20	3.27

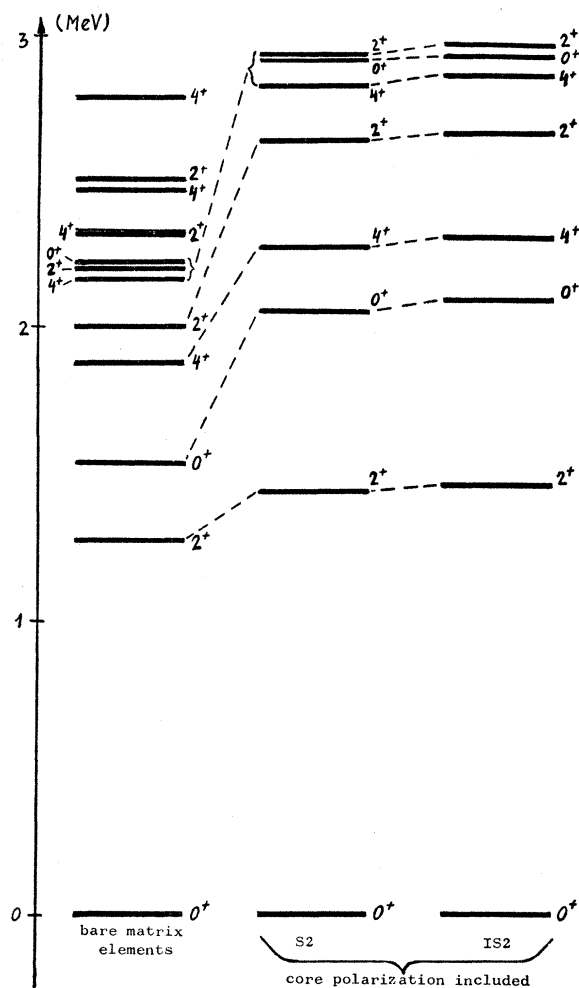


FIG. 2. Spectrum of the lowest-lying 0^+ , 2^+ , and 4^+ energy levels of Sn^{116} calculated in QTD with the Tabakin potential for the single-particle energies $\{E_s^0\}$ Bando 1 of Table I: (1) the matrix elements are bare and only the five valence neutron subshells are involved; (2) differs from (1) by the core polarization included with the (p - h) propagators S2 as in Tables V-VII; (3) differs from (2) by including the core polarization corrections to all orders (case IS2).

and on some quadrupole moments of the 2_1^+ states $Q(2_1^+)$. As far as these latter are concerned, we must stress, however, that, as shown in Ref. 23 coherent contributions of the even small four-qp components of the corresponding QSTD $|2_1^+\rangle$ vectors are usually most important, and any QTD calculation cannot give a satisfactory result. Still, it is interesting to compare the $Q(2_1^+)$ for all our different cases to see the general trends, if any.

In Table VII we present our QTD calculated $B(E2, 2_1^+ \rightarrow 0_1^+)$, $Q(2_1^+)$, the ratio $B(E2, 2_2^+ \rightarrow 0_1^+)/B(E2, 2_1^+ \rightarrow 0_1^+)$ where $2_2^+ \rightarrow 0_1^+$ means the cross-over-to-ground transition from the state 2_2^+ $B(E2, 2_2^+ \rightarrow 2_1^+)$ and $B(E2, 4_1^+ \rightarrow 2_1^+)$, all for the 116 isotope, and for several cases described above. The

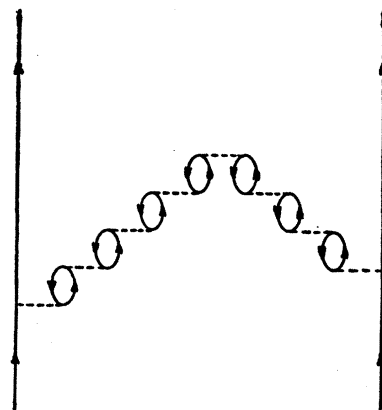


FIG. 3. RPA-type bubble diagrams in the core polarization corrections.

computed values refer to the neutron effective charge $e_n = 1$. Similar results are obtained for $A = 120$.

From Table VII we see that our $B(E2)$ values are generally reasonably stable for all the cases considered and have generally correct trends. The over-all agreement with the existing experimental data is reasonably good for a neutron effective charge e_n close to unity for most of our cases. We note that the required value of e_n is smaller when the core polarization effects are included [the values of $B(E2, 2_1^+ \rightarrow 0_1^+)$ are enhanced by the core renormalization].

Our values of $Q(2_1^+)$ are of the correct sign but too small to explain the large observed²³ $Q(2_1^+, A=116) = +0.4 \pm 0.3$ b. This is because of the fact that, although QTD is able to reproduce the energy of 2_1^+ quite well, the coherent character of the (otherwise not large) components of QSTD is most important in the $Q(2_1^+)$ [actually, $Q(2_1^+)$, as calculated in QSTD, are of the correct order of magnitude.^{7,23}

In our "9+9 levels" calculations with bare matrix elements we find only negligible contributions of the QTD pure proton components to the $B(E2)$ and $Q(2_1^+)$ of Table VII with a proton effective charge of the order unity. Consequently, our results in this case are quite similar to those of Table VII.

4. CONCLUSIONS AND FINAL REMARKS

We have performed a study of the problem of the effects of the core nucleons in two microscopic theories of low-lying excited states of nuclei in the so-called vibrational region on the examples of Sn^{116} and Sn^{120} . The residual nucleon-nucleon interaction was taken in the form of a realistic potential, namely of the nonlocal regular potential of Tabakin. The modification of the BCS pairing force and the extra configuration mixing

²² J. de Boer, in Proceedings of the International Conference on Nuclear Structure, Tokyo, 1967 (to be published).

²³ P. L. Ottaviani, M. Savoia, and J. Sawicki, Nuovo Cimento (to be published).

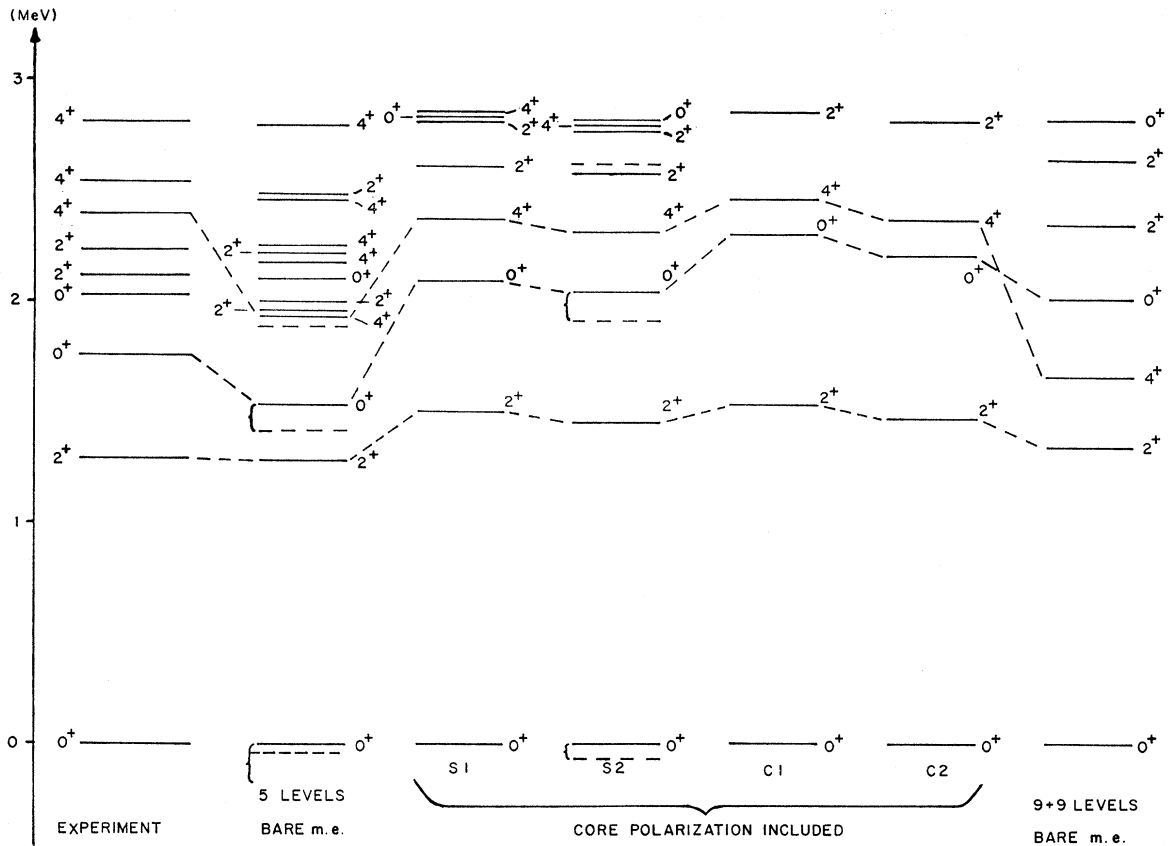


FIG. 4. Energy levels of the states $0_{1,2,3}^+$, $2_{1,2}^+$, and $4_{1,2}^+$ of Sn^{116} ; the QTD and QSTD results refer to the set BEL 1 of Table I and to the cases defined in Tables V-VII; the QSTD 0^+ levels are indicated with broken line.

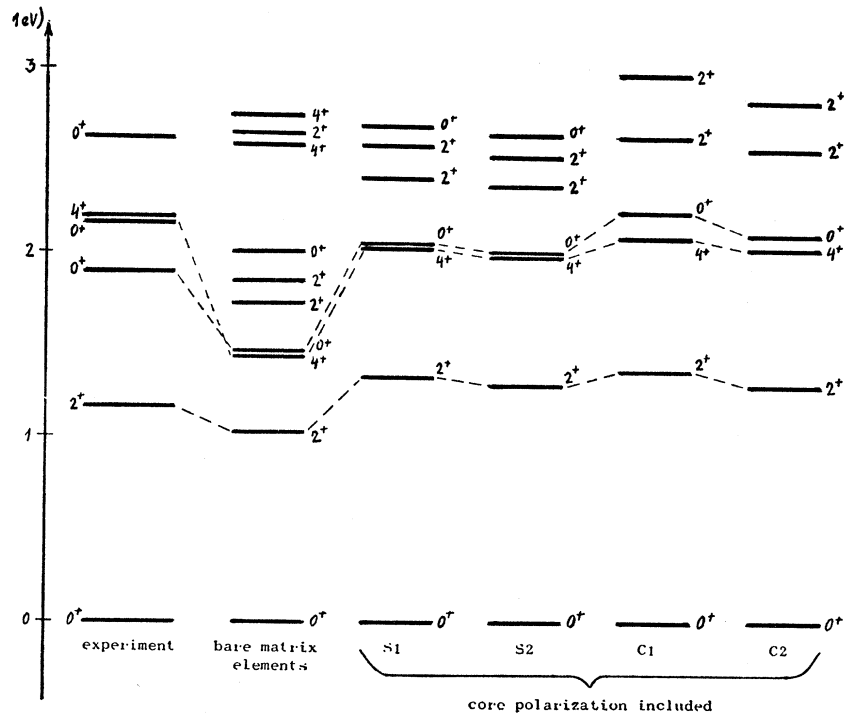


FIG. 5. Energy spectrum of Sn^{120} ; QTD results refer to the set BEL 1 of Table I and to the cases of Tables V-VII.

TABLE VII. $B(E2, I_i \rightarrow I_f)$ (in e^2F^4) and the quadrupole moment $Q(2_1^+)$ (in F^2) of Sn^{116} calculated in QTD with the Tabakin potential with and without the core polarization corrections for the cases defined in Tables V and VI; the neutron effective charge is taken $e_n = 1$.

$e_n = 1$ { E_s^0 }	Matrix elements	$B(E2, 2_1^+ \rightarrow 0_1^+)$ (e^2F^4)	$B(E2, 4_1^+ \rightarrow 2_1^+)$ (e^2F^4)	$B(E2, 2_2^+ \rightarrow 2_1^+)$ (e^2F^4)	$B(E2, 2_2^+ \rightarrow 0_1^+)$		$Q(2_1^+)$ (F^2)
					$B(E2, 2_1^+ \rightarrow 0_1^+)$		
Bando 1	bare	308.0	8.05	5.71	0.007		3.08
	C2	349.1	6.00	2.03	0.027		2.54
	S2	354.9	4.79	2.34	0.010		2.47
	IS2	357.0	4.57	2.05	0.010		2.42
Bando 2	C2	352.0	5.62	2.08	0.020		2.50
	S2	356.8	4.40	2.30	0.007		2.49
BEL 1	bare	287.4	6.13	5.87	$\cong 0$		2.68
	C2	337.2	7.14	3.27	0.018		3.17
	S2	342.8	4.81	3.48	0.002		2.96
BEL 2	C2	340.2	6.53	3.24	0.013		3.13
	S2	344.2	4.20	3.31	0.001		2.98
KBB	bare	215.5	0.66	0.81	0.060		4.43
	C2	292.5	5.67	4.42	0.0005		3.03
	S2	303.8	0.00348	$\cong 0$	$\cong 0$		4.70
	IS2	305.0	0.01	0.004	0.0002		4.66

generated by the excitations of the core neutrons and protons have been taken into account directly in the quasiparticle Tamm-Dancoff (QTD) approximation and through a renormalization of the reduced matrix elements of the nucleon-nucleon interaction between the valence nucleons. The latter procedure, called the core polarization, has been studied including only second-order correction terms and also with the full summation of the Kuo-Brown diagrams to all orders.

We find that the core polarization corrections are generally dramatic and reflect the great importance of excited configurations of core nucleons in microscopic spectroscopy with a realistic potential. In particular, the core corrections lead to important changes of the level densities of low-lying excited states. Reliable quantitative fits to the experimental data call for a single nucleon basis determined with the Hartree-Fock-Bogolyubov self-consistency. In fact, although we are able to fit the data on the 0^+ , 2^+ , and 4^+ states of $\text{Sn}^{116,120}$ if we include the core polarization, we must point out that our results are rather sensitive to the shell-model single-particle energies assumed.

We have found that the inclusion of higher-order bubble and related exchange diagrams leads to only

negligible changes in our results as compared with the case where the core polarization is approximated by the corresponding second-order corrections only.

ACKNOWLEDGMENTS

We are greatly indebted to Dr. P. L. Ottaviani, the author of several of our most important FORTRAN codes for the QTD and QSTD matrix construction and diagonalization, for making them available to us. We are indebted to Professor E. Baranger and to Dr. T. T. S. Kuo for having supplied us with numerical tables of a part of our matrix elements of the Tabakin potential. We have utilized T. K. R. Davies's FORTRAN code for computing the Brody-Moshinsky transformation brackets. Useful discussions with Dr. P. L. Ottaviani and Dr. M. Savoia are acknowledged. We are happy to acknowledge the kind and efficient cooperation of the staff of the IBM 7040 computer of the Centro di Calcolo of the University of Trieste. We express our thanks to Professor Abdus Salam and the IAEA for their hospitality at the International Centre for Theoretical Physics, Trieste. Financial support from UNESCO to one of us (M. G.) is gratefully acknowledged.